Delineating antibody escape from Omicron variants

Henning Gruell[1], Kanika Vanshylla[1], Michael Korenkov[1], Pinkus Tober-Lau[2], Matthias Zehner[1], Friederike Münn[2], Hanna Janicki[1], Max Augustin[3], Philipp Schommers[1,3], Leif Erik Sander[2], Florian Kurth[2,4], Christoph Kreer[1], Florian Klein[1,5,6,*]

1 Laboratory of Experimental Immunology, Institute of Virology, Faculty of Medicine and University Hospital Cologne, University of Cologne, Cologne, Germany
2 Department of Infectious Diseases and Respiratory Medicine, Charité-Universitätsmedizin Berlin, Freie Universität Berlin and Humboldt-Universität zu Berlin, Berlin, Germany
3 Department I of Internal Medicine, Faculty of Medicine and University Hospital Cologne, University of Cologne, Cologne, Germany
4 Department of Tropical Medicine, Bernhard Nocht Institute for Tropical Medicine and Department of Medicine I, University Medical Center Hamburg-Eppendorf, Hamburg, Germany
5 German Center for Infection Research (DZIF), Partner site Bonn-Cologne, Cologne, Germany
6 Center for Molecular Medicine Cologne (CMMC), University of Cologne, Cologne, Germany

* Correspondence should be addressed to florian.klein@uk-koeln.de.

Summary

SARS-CoV-2-neutralizing antibodies play a critical role for protection and treatment of COVID-19. Viral antibody evasion therefore threatens essential prophylactic and therapeutic measures. The high number of mutations in the Omicron BA.1 sublineage results in markedly reduced neutralization susceptibility. Consistently, Omicron is associated with lower vaccine effectiveness and a high re-infection rate. Notably, newly emerging Omicron sublineages (BA.1.1, BA.2) have rapidly become dominant. Here, we determine polyclonal serum activity against BA.1, BA.1.1 and BA.2 in 50 convalescent or vaccinated individuals as well as delineate antibody sensitivities on a monoclonal level using 163 antibodies. Our study reveals a significant but comparable reduction of serum activity against Omicron sublineages which markedly increases after booster immunization. However, notable differences in sensitivity to individual antibodies demonstrate distinct escape patterns of BA.1 and BA.2 that also affect antibodies in clinical use. The results have strong implications for vaccination strategies and antibody use in prophylaxis and therapy.

37 **Introduction**

38 Following its emergence two years into the COVID-19 pandemic, the Omicron variant of
39 SARS-CoV-2 has resulted in a global surge of infections (Viana et al., 2022). Although
40 Omicron is associated with reduced pathogenicity, its high transmissibility poses a
41 considerable threat to individuals at risk and the public health system (Madhi et al., 2022;
42 Meng et al., 2022; Shuai et al., 2022). Moreover, high rates of breakthrough infections in
43 immunized individuals are clinical manifestations of its immune evasive properties
44 (Altarawneh et al., 2022; Andrews et al., 2022; Madhi et al., 2022; Tseng et al., 2022).
45 Omicron's marked resistance to neutralizing antibodies induced by vaccination or
46 previous infection is mediated by a high number of mutations in the spike protein (Cao et
47 al., 2022; Carreno et al., 2022; Cele et al., 2022; Garcia-Beltran et al., 2022; Gruell et al.,
48 2022; Hoffmann et al., 2022; Liu et al., 2022; Planas et al., 2022; Schmidt et al., 2022;
49 VanBlargan et al., 2022). These include mutations that have rendered several therapeutic
50 monoclonal antibodies ineffective (Gruell et al., 2022; Liu et al., 2022; VanBlargan et al.,
51 2022). Prolonged vaccine dosing intervals and booster immunizations based on the
52 ancestral Wu01 strain of SARS-CoV-2 elicit Omicron-neutralizing serum activity (Cheng
53 et al., 2022; Garcia-Beltran et al., 2022; Gruell et al., 2022; Perez-Then et al., 2022; Schmidt
54 et al., 2022; Wratil et al., 2022; Zhao et al., 2022). However, serum titers against Omicron
55 remain lower compared to those against other variants and Omicron breakthrough
56 infections are frequently observed (Kuhlmann et al., 2022). Most experimental evidence
57 on the resistance of the Omicron variant to antibody-mediated neutralization is limited to
58 analyses of the initial BA.1 strain. However, as additional sublineages emerge (Qassim et
59 al., 2022; Yamasoba et al., 2022), determining their escape properties is of critical
60 importance to effectively guide preventive and therapeutic measures. Therefore, we

61 determined in detail antibody-mediated neutralization of the prevalent Omicron
62 sublineages (BA.1, BA.1.1, and BA.2), both on a polyclonal and monoclonal level.
63
64 **Results**
65
66 **Rapid spread of Omicron sublineages**
67 Compared to the Wu01 strain of SARS-CoV-2, the spike protein of BA.1 differs in 39 amino
68 acid residues (**Figure 1A**). While recently emerged sublineages of Omicron share several
69 BA.1 mutations, they differ at various amino acid positions and therefore can alter critical
70 epitopes (**Figures 1A** and **1B**). For example, the spike protein of sublineage BA.1.1
71 contains an additional R346K substitution in the receptor-binding domain (RBD) that was
72 previously observed in the Mu variant of SARS-CoV-2 and has been associated with escape
73 from neutralizing antibodies (**Figure 1A**) (Greaney et al., 2021). Moreover, BA.2 shares
74 only 21 (68%) of its 31 spike protein amino acid changes with BA.1 (**Figure 1A**).
75 Therefore, BA.2 differs considerably from BA.1 and BA.1.1 in both the N-terminal domain
76 (NTD) and the RBD, regions targeted by the most potent SARS-CoV-2-neutralizing
77 antibodies (**Figure 1A**). While BA.1 and BA.1.1 dominated the initial surge of Omicron
78 infections, they have already been outcompeted by BA.2 in numerous countries (**Figure**
79 **1C**). Therefore, the BA.2 omicron sublineage is likely to dominate the SARS-CoV-2
80 pandemic in the near future.
81
82 **Comparable reduction of serum neutralizing activity against Omicron sublineages**
83 We analyzed serum neutralizing activity using lentivirus-based pseudovirus assays
84 against the ancestral Wu01 strain as well as BA.1, BA.1.1, and BA.2 Omicron sublineages
85 (Crawford et al., 2020; Vanshylla et al., 2021). To this end, we collected samples from two

86 longitudinal cohorts of i.) SARS-CoV-2-convalescent individuals (*n*=20) and ii.) vaccinated
87 health care workers (*n*=30) (**Table S1**) (Hillus et al., 2021; Vanshylla et al., 2021). In both
88 cohorts, individuals received an mRNA booster immunization (BNT162b2) after a median
89 of 14 and 9 months following infection or two doses of BNT162b2, respectively.

90 Convalescent individuals had a median age of 51 years (interquartile range [IQR]
91 35-58) and were diagnosed with mild or asymptomatic SARS-CoV-2 infection. Early post-
92 infection samples (V1) were collected at a median of 48 days (IQR 35-58) after disease
93 onset and neutralizing activity was assessed by determining the 50% inhibitory serum
94 dilutions (ID_{50}s) (**Figure 2A**). Neutralization of the Wu01 strain was detected in all
95 samples (100%) obtained early after infection, with individual ID_{50} values ranging from
96 16 to 3,200 (geometric mean ID_{50} [GeoMeanID_{50}] of 322) (**Figure 2B**). In contrast, serum
97 activity against Omicron sublineages was strongly reduced and only detectable in 15%,
98 0%, and 50% for BA.1., BA1.1, and BA.2 respectively (**Figure 2B**). However, following
99 booster immunization at a median of 33 days (IQR 27-54) in convalescent individuals,
100 Omicron-neutralizing activity was elicited in all individuals (**Figures 2B**, **2C**, **S1A** and
101 **S1B**), reaching GeoMeanID_{50}s of 1,688, 1,578, and 2,388 against BA.1, BA.1.1, and BA.2,
102 respectively (**Figure 2B**).

103 In addition, we determined Omicron sublineage-neutralizing activity induced only
104 by vaccination (**Figure 2D**). At a median of 28 days (IQR 27-32) after completion of the
105 initial two-dose course of BNT162b2 (V1), Wu01-neutralizing serum activity was
106 detected in all 30 individuals with a GeoMeanID_{50} of 585 (**Figure 2E**). Although Omicron
107 sublineage-neutralization was detectable in 43-73% of vaccinated individuals,
108 GeoMeanID_{50}s against BA.1, BA.1.1., and BA.2 were low at 11, 8, and 15, respectively
109 (**Figure 2E**). Follow-up samples obtained at a median of 29 days (IQR 26-35) after booster
110 immunization showed 8-fold higher activity against Wu01 (GeoMeanID_{50} of 4,817) and

111 strongly increased Omicron activity in all individuals with GeoMeanID_{50}s of 648 against
112 BA.1, 557 against BA.1.1, and 592 against BA.2 (**Figures 2E**, **S1C**, and **S1D**). We conclude
113 that booster immunizations are critical to elicit neutralizing serum activity against all
114 prevalent Omicron sublineages in vaccinated as well as convalescent individuals. Notably,
115 despite the differences in the spike proteins, Omicron sublineages were similarly affected
116 on the level of serum neutralization.
117

118 **Dissecting viral escape of Omicron sublineages**

119 To decode Omicron escape from neutralizing antibodies, we produced and tested 158
120 monoclonal antibodies isolated from SARS-CoV-2-convalescent individuals against all
121 Omicron sublineages. These included 67 randomly selected antibodies from the CoV-
122 AbDab (Raybould et al., 2021), 79 antibodies isolated in our previous work (Kreer et al.,
123 2020; Vanshylla et al., 2022), as well as 12 clinically evaluated antibodies. In total, this
124 antibody panel originated from at least 43 different individuals out of 19 independent
125 studies (**Figure 3A**, **Table S2**). The selection covered a broad spectrum of diverse SARS-
126 CoV-2 neutralizing antibodies encompassing 92 V_H/V_L combinations. Most of these
127 antibodies targeted the RBD (96.8 %) and included previously described public
128 clonotypes such as the V_H3-53/3-66 subgroup (**Figure 3A**).

129 While all antibodies neutralized the Wu01 strain, only 18%, 17%, and 22%
130 remained active against BA.1, BA.1.1, and BA.2, respectively (**Figure 3B**). Moreover,
131 neutralization against Omicron sublineages was overall lower with GeoMeanIC_{50}s of
132 0.431 (BA.1), 0.506 (BA.1.1), and 0.178 (BA.2) compared to Wu-01-neutralizing
133 antibodies (GeoMeanIC_{50} of 0.030 µg/mL; **Figure 3C**). However, our analysis identified a
134 small number of antibodies with high potency against all Omicron sublineages, including
135 antibodies isolated from individuals with outstanding serum activity (Vanshylla et al.,

136 2022). For example, antibodies R207-2F11 and R568-1G9 both neutralized BA.1, BA.1.1,
137 and BA.2 with IC_{50}s <0.01 μg/ml (**Table S2**). Notably, antibodies maintaining Omicron-
138 neutralizing activity carried a modest but significantly higher (5.2 vs. 6.9) number of V_H
139 amino acid mutations (p=0.002), suggesting that a higher sequence diversification might
140 be favorable for Omicron neutralization (**Figure S2**). Importantly, while antibody
141 neutralization strongly correlated between BA.1 and BA.1.1 (r_s=0.858), a more divergent
142 neutralization profile was observed when comparing BA.1 and BA.2 (r_s=0.763; **Figures**
143 **3D** and **3E**). Based on the analysis of the sublineage neutralization profiles, two prevalent
144 classes of Omicron-neutralizing antibodies became apparent: i.) antibodies with
145 comparable activity against BA.1 and BA.2 lineages (72.5% of antibodies), and ii.)
146 antibodies with higher potency against BA.2 compared to BA.1 (25%) (**Figures 3E**, **3F**,
147 and **3G**). While only a single (2.5%) out of the 40 Omicron-neutralizing antibodies showed
148 >10-fold higher activity against BA.1 than BA.2, 10 out of 40 antibodies showed a 1.1 to
149 3.9 log_{10}-fold higher potency against BA.2 (**Figure 3G**). This indicates that based on the
150 antibody panel tested, immune escape of BA.2 was less pronounced when compared to
151 BA.1 and BA.1.1.

152 Finally, antibody responses against SARS-CoV-2 have previously been
153 demonstrated to be highly convergent across individuals by the identification of several
154 public clonotypes, which are conserved in terms of sequence characteristics and
155 mechanisms of neutralization (Barnes et al., 2020; Nielsen et al., 2020; Robbiani et al.,
156 2020; Yuan et al., 2020). Among the analyzed antibody panel, we identified 18 sequences
157 from 11 individuals that could be assigned to a prominent V_H3-53/3-66|V_K1-9 clonotype
158 (**Figure 3H**) (Cao et al., 2020; Vanshylla et al., 2022; Zhang et al., 2021). Interestingly,
159 although these antibodies are highly conserved on a sequence level, they substantially
160 differed in their Omicron neutralizing capacity (**Figure 3H**). For example, antibodies

161 R207-1C4 and R568-2G5 showed similar neutralizing activity against Wu01 and harbor
162 eight amino acid mutations in their V_H gene segment (without CDRH3) of which five are
163 at the same position and three are identical. However, R207-1C4 was not capable of
164 neutralizing any Omicron variant, while R568-2G5 retained neutralizing activity against
165 all variants. Notably, another member of this clonotype, C140, which has the identical
166 CDRH3 motif as R568-2G5, did not neutralize any Omicron variant. These results indicate
167 that minimal differences in antibody sequence characteristics can tip the scale between
168 Omicron neutralization and resistance.

169 We conclude that the majority of Wu01-neutralizing antibodies lose activity
170 against Omicron sublineages. While most BA.1-neutralizing antibodies were reactive
171 against BA.1.1 and BA.2, the subset of antibodies with Omicron-neutralizing potency
172 restricted towards BA.2 indicates differences in sublineage antigenicity. Moreover, the
173 higher rate of BA.2- compared to BA.1-neutralizing monoclonal antibodies in our panel
174 suggests that the BA.2 spike protein incorporates fewer features associated with
175 resistance.

176

177 **Impact of Omicron sublineages on clinical monoclonal antibodies**

178 SARS-CoV-2-neutralizing monoclonal antibodies can reduce morbidity and mortality in
179 infected individuals. Moreover, they are critical for passive immunization to protect
180 individuals that do not mount an adequate immune response upon vaccination (Cohen et
181 al., 2021; Corti et al., 2021; Dougan et al., 2021; Group, 2022; Gupta et al., 2021; O'Brien
182 et al., 2021; Weinreich et al., 2021). To determine how spike protein mutations of Omicron
183 sublineages affect antibodies in clinical use, we analyzed 9 monoclonal antibodies that
184 received authorization for clinical use (**Figure 4A**) and 9 that are advanced in clinical
185 development (**Figure S3**). All tested antibodies targeted the RBD of the SARS-CoV-2 spike

186 protein and were tested in parallel against Wu01 and the Omicron sublineages (**Figure**
187 **4B**).

188 Most antibodies showed highly potent neutralizing activity against Wu01 with
189 IC_{50}s below 0.005 μg/ml (**Figure 4B**). Less potent and incomplete Wu01-neutralizing
190 activity was observed for sotrovimab, which is consistent with previous reports showing
191 reduced activity against pseudoviruses lacking the dominant D614G spike mutation
192 (**Figure 4A**) (Liu et al., 2021; Weissman et al., 2021). In contrast to the high Wu01 activity,
193 only 5 (28%) out of the 18 tested antibodies neutralized BA.1 with IC_{50}s <10 μg/ml.
194 Moreover, in 2 out of these 5 antibodies, neutralizing activity was decreased by >2 $\log_{10}$
195 against BA.1 relative to Wu01 (**Figure 4B**). While the antibody neutralization profile
196 against the BA.1.1 lineage was generally similar to that of BA.1, a few differences were
197 detected. For example, DZIF-10c neutralized BA.1 with an IC_{50} of 0.046 μg/ml but
198 completely lost activity against BA.1.1 (**Figure 4B**). Although the number of antibodies in
199 clinical use with neutralizing activity against BA.2 remained small (5 out 18, 28%), the
200 neutralization profile of BA.2 differed from that of BA.1 and BA.1.1 (**Figure 4B**). For
201 example, antibody COV2-2130 (cilgavimab) neutralized BA.2 with high potency (IC_{50} of
202 0.008 μg/ml) that was similar to its activity against Wu01 and >800-fold higher than
203 against BA.1 and BA.1.1 (**Figures 4A** and **4B**). In addition, while antibody imdevimab
204 showed no appreciable activity against BA.1 and BA.1.1, neutralization of BA.2 was
205 detectable at low levels (**Figures 4A** and **4B**). Out of all clinical antibodies tested, the
206 recently authorized LY-CoV1404 (bebtelovimab) showed the highest levels of
207 neutralizing activity against all Omicron sublineages (**Figures 4A** and **4B**).

208 We conclude that the prevalent Omicron sublineages are resistant to most
209 monoclonal antibodies in clinical use and/or under investigation. Omicron sensitivity to
210 these antibodies can, however, strongly differ on the sublineage level. Selection of

211 monoclonal antibodies for treatment or prevention of Omicron infection should therefore
212 take sublineage identification and/or epidemiology into account.
213
214 **Discussion**
215 Neutralizing antibody-mediated immunity is a critical component of prophylactic and
216 therapeutic measures against SARS-CoV-2 infection (Corti et al., 2021; Feng et al., 2021;
217 Khoury et al., 2021). The COVID-19 pandemic has been characterized by ongoing viral
218 evolution and periodic emergence of dominant variants in the context of increasing levels
219 of population immunity that can drive selection of antibody resistance (Harvey et al.,
220 2021). Soon after its appearance and explosive spread, considerable immune evasion of
221 the highly mutated BA.1 sublineage of Omicron was confirmed both experimentally and
222 clinically (Altarawneh et al., 2022; Andrews et al., 2022; Cao et al., 2022; Carreno et al.,
223 2022; Cele et al., 2022; Garcia-Beltran et al., 2022; Gruell et al., 2022; Hoffmann et al.,
224 2022; Liu et al., 2022; Madhi et al., 2022; Planas et al., 2022; Schmidt et al., 2022; Tseng et
225 al., 2022; VanBlargan et al., 2022). However, novel Omicron sublineages with differing
226 spike proteins have since become increasingly prevalent, suggesting higher immune
227 escape and/or higher transmissibility (Lyngse et al., 2022; Qassim et al., 2022; Yamasoba
228 et al., 2022). Establishing the impact of the new Omicron sublineages on polyclonal and
229 monoclonal immunity is therefore critical to guide antibody-mediated strategies for
230 prevention and treatment.
231 Our results demonstrate that Wu01-based mRNA vaccine boosters are effective in
232 eliciting activity against the Omicron sublineages and result in comparable neutralizing
233 titers against BA.1, BA.1.1, and BA.2. Although neutralizing activity against Omicron was
234 considerably lower than against the ancestral strain, booster immunizations will
235 therefore continue to be a critical component of vaccination strategies. In addition, our

236 analyses of a large antibody panel revealed similarities and differences in the sensitivity
237 of Omicron sublineages to antibodies isolated from SARS-CoV-2-convalescent individuals.
238 While the resistance profiles of BA.1 and BA.1.1 were largely overlapping, a substantial
239 fraction of antibodies with poor or no BA.1/BA.1.1-neutralizing activity showed high
240 activity against BA.2. Therapeutic monoclonal antibodies authorized for prevention or
241 treatment of SARS-CoV-2 infection were differentially affected, with some showing
242 increased and some showing reduced activity against BA.2 compared to BA.1, confirming
243 similar observations (Iketani et al., 2022). As the majority of tested antibodies failed to
244 neutralize any of the Omicron sublineages, highly potent antibodies identified by our
245 analysis may provide novel options for treatment and prevention in the Omicron era.
246 Our observations of higher pre-boost activity against BA.2, comparable
247 neutralization titers after booster immunization, as well the higher fraction of BA.2- than
248 BA.1-neutralizing monoclonal antibodies isolated from convalescent individuals suggest
249 that BA.2 overall does not have higher levels of antibody escape compared to BA.1.
250 Outcompetition of BA.1 by BA.2 therefore appears to driven rather by higher
251 transmissibility and/or other virological characteristics than by immune evasion.
252 However, as the rapid emergence of the highly resistant Omicron variant illustrated the
253 challenges posed by viral evolution, continuous genomic surveillance and assessments of
254 viral sensitivity will be critical for informing antibody-based prophylactic and therapeutic
255 measures.
256
257 **Acknowledgments**
258 We are grateful to all study participants for their dedication to our research. We thank F.
259 Dewald, L. Gieselmann, B. Kurt, C. Lehmann, P. Mayer, N. Riet, S. Salomon, M. Schlotz, R.
260 Schröder, R. Stumpf and H. Wüstenberg, as well as the members of the EICOV/COVIM

Study Group (Y. Ahlgrimm, L. Bardtke, K. Behn, N. Bethke, H. Bias, D. Briesemeister, C. Conrad, V. M. Corman, C. Dang-Heine, S. Dieckmann, C. Eroglu, D. Frey, J.-A. Gabelich, J. Gerdes, U. Gläser, A. Hetey, L. Hasler, E. T. Helbig, D. Hillus, W. Hirst, A. Horn, C. Hülso, S. Jentzsch, C. von Kalle, L. Kegel, A. Krannich, W. Koch, P. Kopankiewicz, P. Kroneberg, H. Le, L. J. Lippert, C. Lüttke, P. de Macedo Gomes, B. Maeß, C. Matthaiou, J. Michel, A. Nitsche, A.-M. Ollech, C. Peiser, A. Pioch, C. Pley, K. Pohl, C. Rubisch, L. Ruby, A. Sanchez Rezza, I. Schellenberger, V. Schenkel, J. Schlesinger, S. Schmidt, G. Schwanitz, T. Schwarz, J. Seybold, A. Solarek, A. Stege, S. Steinbrecher, P. Stubbemann, C. Thibeault, and D. Treue) for sample acquisition and processing; L. Buchholz and M. Wunsch for help with antibody production and preparation; and J.J. Malin for providing clinical antibody stocks. We thank all laboratories obtaining and submitting SARS-CoV-2 sequencing information to GISAID for facilitating rapid analyses of global variant distributions. This work was supported by grants from COVIM: NaFoUniMedCovid19 (FKZ: 01KX2021) (to L.E.S. and F. Klein), the Federal Institute for Drugs and Medical Devices (V-2021.3 / 1503_68403 / 2021–2022) (to L.E.S. and F. Kurth), the German Center for Infection Research (DZIF) (to F. Klein), and the Deutsche Forschungsgemeinschaft (DFG) CRC1310 (to C.K. and F. Klein).

Author contributions

Conceptualization, H.G., K.V., C.K., and F. Klein; methodology, H.G., K.V., L.E.S., F. Kurth, C.K., and F. Klein; investigation, H.G. and K.V.; resources, P.T-L., M.K., M.Z., F.M., H.J., M.A., and P.S.; formal analysis, H.G., K.V., and C.K.; writing-original draft, H.G., K.V., C.K., and F. Klein; writing-review and editing, M.K., P.T-L., and F. Kurth; visualization, H.G., K.V., C.K., and F. Klein; supervision, L.E.S., F. Kurth, and F. Klein; funding acquisition, L.E.S., F. Kurth, and F. Klein.

286 **Declaration of interests**

287 H.G., K.V., M.Z., C.K., and F. Klein are listed as inventors on patent applications on SARS-
288 CoV-2-neutralizing antibodies encompassing aspects of this work filed by the University
289 of Cologne.

290

291 **Figure legends**

292

293 **Figure 1. Omicron sublineage differences.**

294 **(A)** Spike amino acid changes in the BA.1, BA.1.1, and BA.2 Omicron sublineages relative
295 to Wu01. **(B)** Locations of changed amino acids in Omicron sublineages highlighted on the
296 SARS-CoV-2 spike (PDB: 6XR8). Representations on the right show RBD and NTD outlined
297 in black. Changes exclusive to BA.2 are indicated in dark red (visible on surface) and light
298 red (not visible). In **(A)** and **(B),** mutations shared between BA.1 and BA.1.1 are shown in
299 orange, mutations shared between BA.1, BA.1.1 and BA.2 are shown in blue, the R346K
300 mutation exclusive to BA.1.1 is shown in green, and mutations exclusive to BA.2 are
301 shown in red. **(C)** Proportion of sequences submitted to the GISAID SARS-CoV-2 database
302 per variant and week (accessed on April 2, 2022). NTD, N-terminal domain; RBD,
303 receptor-binding domain; PDB, Protein Data Bank.

304

305 **Figure 2. Omicron sublineage-neutralizing serum activity in vaccinated and**
306 **convalescent individuals.**

307 **(A)** Study scheme in COVID-19-convalescent individuals. Samples were collected after
308 infection occurring between February and April, 2020 (V1), and after a BNT162b2
309 booster immunization (V2). **(B)** Fifty-percent inhibitory serum dilutions (ID_{50}s) against
310 Wu01, BA.1, BA.1.1, and BA.2 determined by pseudovirus neutralization assays in

311 convalescent individuals. Bars indicate geometric mean ID_{50}s with 95% confidence
312 intervals (CIs) at V1 (left) and V2 (right). Numbers indicate geometric mean ID_{50}s and
313 percentage of individuals with detectable neutralizing activity (ID_{50} >10) in parentheses.
314 **(C)** Correlation plots of log_{10} serum ID_{50}s against Wu01 (top) and BA.1 (bottom) versus
315 BA.2 at V2 in convalescent individuals. r_s indicates Spearman's rank correlation
316 coefficients. **(D)** Study scheme in vaccinated individuals. Samples were collected after the
317 second dose of BNT162b2 (V1) and after the third dose of BNT162b2 (V2). **(E)** Serum
318 ID_{50}s against Wu01, BA.1, BA.1.1, and BA.2 determined by pseudovirus neutralization
319 assays in vaccinated individuals. Bars indicate geometric mean ID_{50}s with 95% CIs at V1
320 (left) and V2 (right). Numbers indicate geometric mean ID_{50}s and percentage of
321 individuals with detectable neutralizing activity (ID_{50} >10) in parentheses. **(F)** Correlation
322 plots of log_{10} serum ID_{50}s against Wu01 (top) and BA.1 (bottom) versus BA.2 at V2 in
323 vaccinated individuals. r_s indicates Spearman's rank correlation coefficients. In **(B)** and
324 **(E)**, ID_{50}s below the lower limit of quantification (LLOQ, ID_{50} of 10; indicated by black
325 dotted lines) were imputed to ½ LLOQ (ID_{50}=5). In **(B)** and **(C)**, ID_{50}s above the upper
326 limit of quantification (21,870) were imputed to 21,871.
327
328 **Figure 3. Determining Omicron sublineage immune escape using monoclonal**
329 **antibodies.**
330 **(A)** SARS-CoV-2-neutralizing monoclonal antibodies (*n*=158) derived from 19 studies and
331 isolated from ≥43 convalescent individuals were analyzed. Bar charts indicate number of
332 antibodies per heavy chain variable gene segment (V_H), amino acid (aa) length of the
333 heavy chain complementarity-determining region 3 (CDRH3), and number of V_H aa
334 mutations relative to the V_H germline gene. Pie chart indicates antibody epitopes with
335 slice sizes proportional to the number of antibodies. **(B)** Fraction of monoclonal

336 antibodies neutralizing (IC_{50} <10 μg/ml) Wu01 (green), BA.1 (light red), BA.1.1 (dark
337 red), and BA.2 (blue) in pseudovirus neutralization assay. **(C)** IC_{50}s of antibodies with
338 neutralizing activity (IC_{50} <10 μg/ml) against the individual variants (Wu01, *n*=158; BA.1,
339 *n*=29; BA.1.1, *n=27*; BA.2, *n=34*). Bars depict geometric mean IC_{50}s and dotted line
340 indicates lower limit of quantification (LLOQ, 0.005 μg/ml). **(D)** Spider plot of IC_{50}s for all
341 antibodies against Wu01, BA.1, BA.1.1, and BA.2. Antibodies are sorted arbitrarily but
342 equally for each virus. **(E)** Correlation plots of IC_{50}s of all antibodies against BA.1.1 (left)
343 and BA.2 (right) versus BA.1. Colors indicate epitopes as in (**A**). Dashed lines represent
344 identity lines and dotted lines indicate limits of quantification. **(F)** Bar charts of antibodies
345 with neutralizing activity (IC_{50} <10 μg/ml) against any Omicron sublineage (*n*=40).
346 Antibodies in each chart are sorted by BA.1-neutralizing activity (black outline) and bars
347 show IC_{50}s against indicated sublineages. Dotted lines show LLOQ (0.005 μg/ml) and
348 upper limit of quantification (ULOQ; 10 μg/ml). **(G)** Ratio (log_{10}) of IC_{50}s against BA.1 and
349 BA.2 for all neutralizing antibodies with any Omicron sublineage-neutralizing activity
350 (IC_{50} <10 μg/ml; *n*=40). Ratios >1 log_{10} are highlighted in green and percentage of
351 antibodies with ratio >1 log_{10} is indicated. In **(E)-(G)**, IC_{50} <LLOQ were imputed to ½ LLOQ
352 (IC_{50}=0.0025) and IC_{50} values >ULOQ were imputed to 2x ULOQ (IC_{50}=20). **(H)**
353 Phylogenetic tree and sequence alignment of antibodies of the V_H3-53/3-66|V_K1-9 public
354 clonotype. Letters indicate aa mutations relative to the V_H germline gene. Number of aa
355 mutations compared to the corresponding germline allele and neutralizing activity
356 against Wu01, BA.1, BA.1.1, and BA.2 are indicated on the right. Germline V_H represents
357 the consensus of all identified germline alleles of depicted antibodies (V_H3-53*01, V_H3-
358 53*04, and V_H3-66*01).
359

360 **Figure 4. Omicron sublineage-neutralizing activity of monoclonal antibodies in**
361 **clinical use.**
362 **(A)** Dose response curves showing % neutralization of monoclonal antibodies against
363 Wu01, BA.1, BA.1.1, and BA.2 in pseudovirus neutralization assay. Circles show averages
364 and error bars indicate standard deviation. Dotted lines indicate 50% neutralization
365 (IC_{50}). (**B**) IC_{50}s against Wu01, BA.1, BA.1.1, and BA.2 of monoclonal antibodies with
366 current or previous authorization for clinical use or in clinical development. Symbols
367 indicate whether clinical products or parental antibodies produced as human IgG1 were
368 used.
369
370 **Supplementary figure legends**
371
372 **Figure S1. Serum neutralization of Omicron sublineages.**
373 **(A)** Serum ID_{50}s against Wu01, BA.1, BA.1.1, and BA.2 in the cohort of convalescent
374 individuals after infection (V1) and BNT162b2 booster immunization (V2) as in **Figure 2**.
375 Lines connect ID_{50}s of individual participants at V1 and V2. (**B**) Correlation plots of $\log_{10}$
376 serum ID_{50}s against indicated viruses in convalescent individuals at V2. r_s indicates
377 Spearman's rank correlation coefficients. **(C)** Serum ID_{50}s against Wu01, BA.1, BA.1.1, and
378 BA.2 in the cohort of BNT162b2-vaccinated individuals after the second (V1) and the
379 third vaccine dose (V2) as in **Figure 2**. Lines connect ID_{50}s of individual participants at V1
380 and V2. **(D)** Correlation plots of $\log_{10}$ serum ID_{50}s against indicated viruses in vaccinated
381 individuals at V2. r_s indicates Spearman's rank correlation coefficients.
382
383
384

385 **Figure S2. Sequence mutations in Omicron-neutralizing antibodies.**

386 Number of antibody V_H amino acid mutations compared to V_H germline sequence for
387 antibodies not neutralizing (IC_{50} >10 µg/ml) any of the Omicron sublineages (left) or
388 neutralizing at least one of the Omicron sublinages (right). Lines indicate mean and error
389 bars indicate standard deviation. Statistical significance was determined using a two-
390 sided Mann-Whitney U test.

391

392 **Figure S3. Omicron sublineage-neutralizing activity of monoclonal antibodies in**
393 **clinical testing.**

394 Dose response curves showing % neutralization of monoclonal antibodies against
395 Wu01, BA.1, BA.1.1, and BA.2 in a pseudovirus neutralization assay. Circles show
396 averages and error bars indicate standard deviation. Dotted lines indicate 50%
397 neutralization (IC_{50}).

398

399 **Supplementary tables**

400 **Table S1**: Study cohorts

401 **Table S2:** Monoclonal antibody panel analyses

402

403 **Methods**

404

405 **Study cohort and sample collection**

406 Serum samples from COVID-19-convalescent individuals were collected at the University
407 Hospital Cologne under study protocols approved by the ethics committee (EC) of the
408 Medical Faculty of the University of Cologne (16-054 and 20-1187). Between April and
409 May, 2020, individuals with a history of SARS-CoV-2 infection confirmed by polymerase

410 chain reaction (documented through a written test certificate or as reported to study
411 investigators by the participants) were enrolled within eight weeks of symptom onset
412 and/or diagnosis. As all participants were enrolled early during the pandemic (i.e., prior
413 to the emergence of variants of concern, as designated by the World Health Organization),
414 most individuals are likely to have been infected with an early viral strain similar to Wu01.
415 Participants were followed longitudinally to analyze long-term immunity to SARS-CoV-2.
416 Serum samples from vaccinated individuals were collected under protocols
417 approved by the EC of Charité - Universitätsmedizin Berlin (EICOV, EA4/245/20) as well
418 as the EC of the Federal State of Berlin and the Paul Ehrlich Institute (COVIM, EudraCT-
419 No. 2021-001512-28). Study participation irrespective of medical conditions was offered
420 to health-care workers vaccinated at the Charité – Universitätsmedizin (Berlin, Germany).
421 All serum samples were tested for antibodies targeting the SARS-CoV-2 nucleocapsid
422 using the SeraSpot Anti-SARS-CoV-2 IgG microarray-based immunoassay (Seramun
423 Diagnostica). Samples from individuals with a history of SARS-CoV-2 infection, a positive
424 SARS-CoV-2 nucleic acid amplification test (performed at sampling), or detectable anti-
425 nucleocapsid antibodies were not included in this analysis.
426 All study participants provided written informed consent. Vaccinations in both
427 cohorts were performed as part of routine care outside of the observational studies.
428 Selection of participants and samples for analysis was based on receipt of identical
429 vaccines and comparable sampling time points relative to vaccinations. Serum samples
430 were collected after centrifugation and stored at -80°C until analysis.
431
432 **SARS-CoV-2 pseudovirus constructs**
433 All SARS-CoV-2 spike proteins were expressed using codon-optimized expression
434 plasmids. Wu01 (EPI_ISL_406716) pseudoviruses were produced using an expression

435 plasmid that incorporated a C-terminal deletion of 21 cytoplasmic amino acids that result
436 in increased pseudovirus titers. Expression plasmids for Omicron sublinage spike
437 proteins were produced by assembling and cloning codon-optimized overlapping gene
438 fragments (Thermo Fisher) into the pCDNA3.1/V5-HisTOPO vector (Thermo Fisher)
439 using the NEBuilder HiFi DNA Assembly Kit (New England Biolabs), and included the full
440 spike protein amino acid sequences with the following amino acid changes relative to
441 Wu01:
442 BA.1: A67V, Δ69-70, T95I, G142D, Δ143-145, N211I, Δ212, ins215EPE, G339D, S371L,
443 S373P, S375F, K417N, N440K, G446S, S477N, T478K, E484A, Q493R, G496S, Q498R,
444 N501Y, Y505H, T547K, D614G, H655Y, N679K, P681H, N764K, D796Y, N856K, Q954H,
445 N969K, and L981F.
446 BA.1.1: As for BA.1 with an additional R346K mutation.
447 BA.2: T19I, Δ24-26, A27S, A67V, G142D, V213G, G339D, S371F, S373P, S375F, T376A,
448 D405N, R408S, K417N, N440K, S477N, T478K, E484A, Q493R, Q498R, N501Y, Y505H,
449 D614G, H655Y, N679K, P681H, N764K, D796Y, Q954H, N969K.
450 All plasmid sequences were verified by sequencing.
451
452 **Monoclonal antibodies**
453 Monoclonal antibodies previously isolated in our lab had been obtained by single cell-
454 sorting of SARS-CoV-2 spike-specific B cells followed by reverse transcription, PCR
455 amplification and cloning of antibody variable regions (Kreer et al., 2020; Vanshylla et al.,
456 2022). For monoclonal antibodies derived from the CoV-AbDab (Raybould et al., 2021),
457 variable region amino acid sequences were reverse translated with the reverse translate
458 tool from the Sequence Manipulation Suite (Stothard, 2000) using the *Homo sapiens*
459 codon table obtained from the Codon Usage Database (Nakamura et al., 2000), and

460 sequences were ordered as gene fragments from Integrated DNA Technologies (IDT) with
461 5' and 3' overhangs. The variable regions were inserted into heavy and light chain
462 expression plasmids (Tiller et al., 2008) by sequence- and ligation-independent cloning
463 (SLIC). For antibodies ADG-2, COV2-2130, COV2-2196, COV2-2381, MAD0004J08, and
464 P2C-1F11, gene fragments based on the nucleotide sequences published in GenBank were
465 ordered at IDT and cloned as above. For antibodies C135, CT-P59, and LY-CoV1404, gene
466 fragments based on antibody structures deposited in the Protein Data Bank (accession
467 nos. 7K8Z, 7CM4, and 7MMO) were ordered at IDT after codon optimization using the IDT
468 Codon Optimization Tool and cloned as above. For antibodies 47D11, BD-368-2, C144,
469 and P2B-2F6, amino acid sequences were derived from CoV-AbDaB, corresponding
470 nucleotide sequences generated and codon-optimized using the IDT Codon Optimization
471 Tool, and gene fragments cloned as above.
472 Monoclonal antibody production was performed using 293-6E cells (National
473 Research Council of Canada) by co-transfection of heavy and light chain expression
474 plasmids using 25 kDa branched polyethylenimine (Sigma-Aldrich). Culture supernatants
475 were harvested after an incubation period of 6-7 days at 37°C and 6% CO2 under constant
476 shaking in FreeStyle Expression Medium supplemented with penicillin (20 U/ml) and
477 streptomycin (20 μg/ml) (all Thermo Fisher). Clarified cell supernatants were incubated
478 with Protein G Sepharose 4 FastFlow (Cytiva) overnight at 4°C . After centrifugation,
479 antibodies bound to Protein G beads were eluted in chromatography columns (Bio-Rad)
480 using 0.1 M glycine (pH=3.0) and buffered in 1 M Tris (pH=8.0). Buffer exchange to PBS
481 was performed using centrifugal filter units (Millipore). For antibodies bamlanivimab,
482 casirivimab, DZIF-10c, etesevimab, imdevimab, and sotrovimab, aliquots from clinical
483 stocks were used.
484

485 **Pseudovirus neutralization assays**

486 Neutralization assays were performed using lentivirus-based pseudoviruses and ACE2-
487 expressing 293T cells (Crawford et al., 2020; Vanshylla et al., 2021). Pseudovirus particle
488 production was performed in HEK293T cells by co-transfection of individual expression
489 plasmids encoding for the SARS-CoV-2 spike protein, HIV-1 Tat, HIV-1 Gag/Pol, HIV-1 Rev,
490 and luciferase-IRES-ZsGreen using FuGENE 6 Transfection Reagent (Promega). Culture
491 supernatants were exchanged with fresh medium (high glucose DMEM supplemented
492 with 2 mM L-glutamine, 100 IU/ml penicillin, 100 µg/ml streptomycin, 1 mM sodium
493 pyruvate (all Thermo Fisher), and 10% FBS (Sigma-Aldrich)) 24 h post transfection.
494 Pseudovirus-containing supernatants were harvested between 48-72 h after transfection,
495 centrifuged, clarified using a 0.45 µm filter, and stored at -80°C. Pseudoviruses were
496 titrated by infection of 293T-ACE2 cells and luciferase activity was determined after a 48-
497 hour incubation at 37°C and 5% CO_2 by addition of luciferin/lysis buffer (10 mM $MgCl_2$,
498 0.3 mM ATP, 0.5 mM coenzyme A, 17 mM IGEPAL CA-630 (all Sigma-Aldrich), and 1 mM
499 D-Luciferin (GoldBio) in Tris-HCL) using a microplate reader (Berthold).

500 Serum samples were heat-inactivated at 56°C for 45 min before use. Three-fold
501 serial dilutions of serum (starting at 1:10) and monoclonal antibodies (starting at 10
502 µg/ml) were prepared in culture medium and co-incubated with pseudovirus
503 supernatants for one hour at 37°C and 5% CO_2 prior to addition of 293T-ACE2 cells.
504 Following a 48-hour incubation at 37°C and 5% CO_2, luciferase activity was determined
505 as described above. Average background relative light units (RLUs) of non-infected cells
506 were subtracted, and serum ID_{50}s and antibody IC_{50}s were determined as the serum
507 dilutions and antibody concentrations resulting in a 50% RLU reduction compared to the
508 average of virus-infected untreated controls cells using a non-linear fit model plotting an
509 agonist vs. normalized dose response curve with variable slope using the least squares

510 fitting method in Prism 7.0 (GraphPad). All serum and monoclonal antibody samples were
511 tested in duplicates. Imputation rules for values outside the limits of quantification are
512 described below (see Statistical methods).
513
514 **SARS-CoV-2 neutralizing antibody panel and sequence analysis**
515 The panel of 158 SARS-CoV-2-neutralizing monoclonal antibodies isolated from SARS-
516 CoV-2 convalescent individuals included in the analysis in **Figure 3** is based on 79
517 antibodies obtained in our previous work (Kreer et al., 2020; Vanshylla et al., 2022), 67
518 randomly selected (retrieved on January 1, 2021) human SARS-CoV-2-neutralizing
519 antibodies deposited at CoV-AbDab (Raybould et al., 2021), and 12 antibodies in clinical
520 use or development. We did not include five of the antibodies in clinical development
521 shown in **Figure 4** into this analysis, as they were obtained from individuals infected with
522 SARS-CoV (ADG-2, sotrovimab), from immunized mice harboring human immunglobulin
523 gene repertoires (47D11, casirivimab), or using phage display technology that does not
524 ensure native pairing of antibody heavy and light chains (CT-P59). For antibody DZIF-10c,
525 the parental antibody (HbnC3t1p1_F4) was included in the analysis in **Figure 3**, while the
526 clinical product is included in **Figure 4**.
527 Antibody amino acid sequences were annotated with IgBLASTp (Ye et al., 2013)
528 based on the IMGT database (Lefranc, 2011). For sequence statistics, top V gene calls were
529 counted without individual alleles, CDR3 lengths are reported according to the IMGT
530 numbering system and numbers of V_H mutations refer to the top V gene call from
531 IgBLASTp. Phylogenetic analysis of antibodies belonging to the V_H3-53/3-66|V_K1-9 public
532 clonotype was performed by alignment of amino acid sequences with the MAFFT
533 algorithm (Katoh et al., 2002) via the EMBL-EBI search and sequence analysis tools API
534 (Madeira et al., 2019) and the Tree Builder tool from Geneious Prime 2020.0.4

535 (Biomatters) using the Jukes-Cantor distance model for tree building with the neighbour-
536 joining method without resampling. Data aggregation and visualization was performed
537 with the Python libraries pandas (v1.1.5), NumPy (v1.19.2), SciPy (v1.5.2), Matplotlib
538 (v3.3.4) with Python (v3.6.8), as well as Microsoft Excel 2011 for Mac (v14.7.3), and
539 Adobe Illustrator.
540
541 **Visualization of SARS-CoV-2 spike amino acid changes**
542 Amino acid changes relative to the Wu01 spike protein were visualized on a cryo-electron
543 microscopy 3D-reconstruction of the SARS-CoV-2 spike protein (PDB ID: 6XR8) (Cai et al.,
544 2020) using ChimeraX (v. 1.3) (Goddard et al., 2018; Pettersen et al., 2021).
545
546 **SARS-CoV-2 variant distribution**
547 GISAID-curated clade and lineage statistics of sequences submitted to the GISIAD
548 database (Elbe and Buckland-Merrett, 2017; Khare et al., 2021; Shu and McCauley, 2017)
549 were retrieved from GISAID (accessed on April 2, 2022) and frequency of individual
550 variants was plotted as fraction of all submitted sequences per week and variant.
551
552 **Statistical Methods**
553 For graphical representation and statistical evaluation of serum samples in **Figures 2** and
554 **S1**, samples that did not achieve 50% inhibition at the lowest tested dilution of 10 (lower
555 limit of quantification, LLOQ) were imputed to ½ of the LLOQ (ID_{50}=5) and serum samples
556 with ID_{50} >21,870 (upper limit of quantification) were imputed to ID_{50}=21871. For
557 graphical representation and statistical analysis of monoclonal neutralizing antibodies in
558 **Figure 3**, IC_{50} values of antibodies with an IC_{50} <0.005 µg/ml (LLOQ) were imputed to ½
559 LLOQ (IC_{50}=0.0025) and IC_{50} values >10 µg/ml (ULOQ) were imputed to 2x ULOQ (IC_{50}=20

560 μg/ml). Spearman's rank correlation coefficients were determined using Prism 7.0
561 (GraphPad; serum samples) or the spearmanr() function of the SciPy-package (v 1.5.2)
562 stats-module (monoclonal antibodies). For the comparison of the number of V_H amino
563 acid mutations relative to germline between antibodies neutralizing Wu01 or any
564 Omicron sublineage, a two-sided Mann-Whitney U test was performed using the
565 mannwhitneyu() function of the SciPy-package (v 1.5.2) stats-module.
566

567 **Data and code availability**

568 Requests for data or materials should be directed to the corresponding author and may
569 be subject to restrictions based on data and privacy protection regulations and/or may
570 require a Material Transfer Agreement (MTA). The paper does not report original code.
571

572 **References**

573 Altarawneh, H.N., Chemaitelly, H., Hasan, M.R., Ayoub, H.H., Qassim, S., AlMukdad, S., Coyle,
574 P., Yassine, H.M., Al-Khatib, H.A., Benslimane, F.M., et al. (2022). Protection against the
575 Omicron Variant from Previous SARS-CoV-2 Infection. N Engl J Med.

576 Andrews, N., Stowe, J., Kirsebom, F., Toffa, S., Rickeard, T., Gallagher, E., Gower, C., Kall, M.,
577 Groves, N., O'Connell, A.-M., et al. (2022). Covid-19 Vaccine Effectiveness against the
578 Omicron (B.1.1.529) Variant. New England Journal of Medicine.

579 Barnes, C.O., West, A.P., Jr., Huey-Tubman, K.E., Hoffmann, M.A.G., Sharaf, N.G., Hoffman,
580 P.R., Koranda, N., Gristick, H.B., Gaebler, C., Muecksch, F., et al. (2020). Structures of Human
581 Antibodies Bound to SARS-CoV-2 Spike Reveal Common Epitopes and Recurrent Features
582 of Antibodies. Cell 182, 828-842 e816.

583 Cai, Y., Zhang, J., Xiao, T., Peng, H., Sterling, S.M., Walsh, R.M., Jr., Rawson, S., Rits-Volloch,
584 S., and Chen, B. (2020). Distinct conformational states of SARS-CoV-2 spike protein.
585 Science 369, 1586-1592.

586 Cao, Y., Su, B., Guo, X., Sun, W., Deng, Y., Bao, L., Zhu, Q., Zhang, X., Zheng, Y., Geng, C., et al.
587 (2020). Potent Neutralizing Antibodies against SARS-CoV-2 Identified by High-
588 Throughput Single-Cell Sequencing of Convalescent Patients' B Cells. Cell 182, 73-84 e16.

589 Cao, Y., Wang, J., Jian, F., Xiao, T., Song, W., Yisimayi, A., Huang, W., Li, Q., Wang, P., An, R.,
590 et al. (2022). Omicron escapes the majority of existing SARS-CoV-2 neutralizing
591 antibodies. Nature 602, 657-663.

592 Carreno, J.M., Alshammary, H., Tcheou, J., Singh, G., Raskin, A.J., Kawabata, H., Sominsky,
593 L.A., Clark, J.J., Adelsberg, D.C., Bielak, D.A., et al. (2022). Activity of convalescent and
594 vaccine serum against SARS-CoV-2 Omicron. Nature 602, 682-688.

595 Cele, S., Jackson, L., Khoury, D.S., Khan, K., Moyo-Gwete, T., Tegally, H., San, J.E., Cromer, D.,
596 Scheepers, C., Amoako, D.G., et al. (2022). Omicron extensively but incompletely escapes
597 Pfizer BNT162b2 neutralization. Nature 602, 654-656.

598 Cheng, S.M.S., Mok, C.K.P., Leung, Y.W.Y., Ng, S.S., Chan, K.C.K., Ko, F.W., Chen, C., Yiu, K.,
599 Lam, B.H.S., Lau, E.H.Y., et al. (2022). Neutralizing antibodies against the SARS-CoV-2
600 Omicron variant BA.1 following homologous and heterologous CoronaVac or BNT162b2
601 vaccination. Nat Med.

602 Cohen, M.S., Nirula, A., Mulligan, M.J., Novak, R.M., Marovich, M., Yen, C., Stemer, A., Mayer,
603 S.M., Wohl, D., Brengle, B., et al. (2021). Effect of Bamlanivimab vs Placebo on Incidence of
604 COVID-19 Among Residents and Staff of Skilled Nursing and Assisted Living Facilities: A
605 Randomized Clinical Trial. JAMA 326, 46-55.

606 Corti, D., Purcell, L.A., Snell, G., and Veesler, D. (2021). Tackling COVID-19 with
607 neutralizing monoclonal antibodies. Cell 184, 3086-3108.

608 Crawford, K.H.D., Eguia, R., Dingens, A.S., Loes, A.N., Malone, K.D., Wolf, C.R., Chu, H.Y.,
609 Tortorici, M.A., Veesler, D., Murphy, M., et al. (2020). Protocol and Reagents for
610 Pseudotyping Lentiviral Particles with SARS-CoV-2 Spike Protein for Neutralization
611 Assays. Viruses 12.

612 Dougan, M., Nirula, A., Azizad, M., Mocherla, B., Gottlieb, R.L., Chen, P., Hebert, C., Perry, R.,
613 Boscia, J., Heller, B., et al. (2021). Bamlanivimab plus Etesevimab in Mild or Moderate
614 Covid-19. N Engl J Med 385, 1382-1392.

615 Elbe, S., and Buckland-Merrett, G. (2017). Data, disease and diplomacy: GISAID's
616 innovative contribution to global health. Glob Chall 1, 33-46.

617 Feng, S., Phillips, D.J., White, T., Sayal, H., Aley, P.K., Bibi, S., Dold, C., Fuskova, M., Gilbert,
618 S.C., Hirsch, I., et al. (2021). Correlates of protection against symptomatic and
619 asymptomatic SARS-CoV-2 infection. Nat Med 27, 2032-2040.

620 Garcia-Beltran, W.F., St Denis, K.J., Hoelzemer, A., Lam, E.C., Nitido, A.D., Sheehan, M.L.,
621 Berrios, C., Ofoman, O., Chang, C.C., Hauser, B.M., et al. (2022). mRNA-based COVID-19
622 vaccine boosters induce neutralizing immunity against SARS-CoV-2 Omicron variant. Cell
623 185, 457-466 e454.

624 Goddard, T.D., Huang, C.C., Meng, E.C., Pettersen, E.F., Couch, G.S., Morris, J.H., and Ferrin,
625 T.E. (2018). UCSF ChimeraX: Meeting modern challenges in visualization and analysis.
626 Protein Sci 27, 14-25.

627 Greaney, A.J., Starr, T.N., Barnes, C.O., Weisblum, Y., Schmidt, F., Caskey, M., Gaebler, C.,
628 Cho, A., Agudelo, M., Finkin, S., et al. (2021). Mapping mutations to the SARS-CoV-2 RBD
629 that escape binding by different classes of antibodies. Nat Commun 12, 4196.

630 Group, R.C. (2022). Casirivimab and imdevimab in patients admitted to hospital with
631 COVID-19 (RECOVERY): a randomised, controlled, open-label, platform trial. The Lancet
632 399, 665-676.

633 Gruell, H., Vanshylla, K., Tober-Lau, P., Hillus, D., Schommers, P., Lehmann, C., Kurth, F.,
634 Sander, L.E., and Klein, F. (2022). mRNA booster immunization elicits potent neutralizing
635 serum activity against the SARS-CoV-2 Omicron variant. Nat Med.

636 Gupta, A., Gonzalez-Rojas, Y., Juarez, E., Crespo Casal, M., Moya, J., Falci, D.R., Sarkis, E.,
637 Solis, J., Zheng, H., Scott, N., et al. (2021). Early Treatment for Covid-19 with SARS-CoV-2
638 Neutralizing Antibody Sotrovimab. N Engl J Med 385, 1941-1950.

639 Harvey, W.T., Carabelli, A.M., Jackson, B., Gupta, R.K., Thomson, E.C., Harrison, E.M.,
640 Ludden, C., Reeve, R., Rambaut, A., Consortium, C.-G.U., et al. (2021). SARS-CoV-2 variants,
641 spike mutations and immune escape. Nat Rev Microbiol 19, 409-424.

642 Hillus, D., Schwarz, T., Tober-Lau, P., Vanshylla, K., Hastor, H., Thibeault, C., Jentzsch, S.,
643 Helbig, E.T., Lippert, L.J., Tscheak, P., et al. (2021). Safety, reactogenicity, and
644 immunogenicity of homologous and heterologous prime-boost immunisation with
645 ChAdOx1 nCoV-19 and BNT162b2: a prospective cohort study. The Lancet Respiratory
646 Medicine 9, 1255-1265.

647 Hoffmann, M., Kruger, N., Schulz, S., Cossmann, A., Rocha, C., Kempf, A., Nehlmeier, I.,
648 Graichen, L., Moldenhauer, A.S., Winkler, M.S., et al. (2022). The Omicron variant is highly
649 resistant against antibody-mediated neutralization: Implications for control of the COVID-
650 19 pandemic. Cell 185, 447-456 e411.

651 Iketani, S., Liu, L., Guo, Y., Liu, L., Chan, J.F.W., Huang, Y., Wang, M., Luo, Y., Yu, J., Chu, H., et
652 al. (2022). Antibody evasion properties of SARS-CoV-2 Omicron sublineages. Nature.

653 Katoh, K., Misawa, K., Kuma, K., and Miyata, T. (2002). MAFFT: a novel method for rapid
654 multiple sequence alignment based on fast Fourier transform. Nucleic Acids Res 30, 3059-
655 3066.

656 Khare, S., Gurry, C., Freitas, L., Schultz, M.B., Bach, G., Diallo, A., Akite, N., Ho, J., Lee, R.T.,
657 Yeo, W., et al. (2021). GISAID's Role in Pandemic Response. China CDC Wkly 3, 1049-1051.

658 Khoury, D.S., Cromer, D., Reynaldi, A., Schlub, T.E., Wheatley, A.K., Juno, J.A., Subbarao, K.,
659 Kent, S.J., Triccas, J.A., and Davenport, M.P. (2021). Neutralizing antibody levels are highly
660 predictive of immune protection from symptomatic SARS-CoV-2 infection. Nat Med 27,
661 1205-1211.

662 Kreer, C., Zehner, M., Weber, T., Ercanoglu, M.S., Gieselmann, L., Rohde, C., Halwe, S.,
663 Korenkov, M., Schommers, P., Vanshylla, K., et al. (2020). Longitudinal Isolation of Potent
664 Near-Germline SARS-CoV-2-Neutralizing Antibodies from COVID-19 Patients. Cell 182,
665 843-854 e812.

666 Kuhlmann, C., Mayer, C.K., Claassen, M., Maponga, T., Burgers, W.A., Keeton, R., Riou, C.,
667 Sutherland, A.D., Suliman, T., Shaw, M.L., et al. (2022). Breakthrough infections with SARS-
668 CoV-2 omicron despite mRNA vaccine booster dose. The Lancet 399, 625-626.

669 Lefranc, M.P. (2011). IMGT, the International ImMunoGeneTics Information System. Cold
670 Spring Harb Protoc 2011, 595-603.

671 Liu, C., Ginn, H.M., Dejnirattisai, W., Supasa, P., Wang, B., Tuekprakhon, A., Nutalai, R., Zhou,
672 D., Mentzer, A.J., Zhao, Y., et al. (2021). Reduced neutralization of SARS-CoV-2 B.1.617 by
673 vaccine and convalescent serum. Cell 184, 4220-4236 e4213.

674 Liu, L., Iketani, S., Guo, Y., Chan, J.F., Wang, M., Liu, L., Luo, Y., Chu, H., Huang, Y., Nair, M.S.,
675 et al. (2022). Striking antibody evasion manifested by the Omicron variant of SARS-CoV-
676 2. Nature 602, 676-681.

677 Lyngse, F.P., Kirkeby, C.T., Denwood, M., Christiansen, L.E., Mølbak, K., Møller, C.H., Skov,
678 R.L., Krause, T.G., Rasmussen, M., Sieber, R.N., et al. (2022). Transmission of SARS-CoV-2
679 Omicron VOC subvariants BA.1 and BA.2: Evidence from Danish Households. medRxiv.

680 Madeira, F., Park, Y.M., Lee, J., Buso, N., Gur, T., Madhusoodanan, N., Basutkar, P., Tivey,
681 A.R.N., Potter, S.C., Finn, R.D., et al. (2019). The EMBL-EBI search and sequence analysis
682 tools APIs in 2019. Nucleic Acids Res 47, W636-W641.

683 Madhi, S.A., Kwatra, G., Myers, J.E., Jassat, W., Dhar, N., Mukendi, C.K., Nana, A.J., Blumberg,
684 L., Welch, R., Ngorima-Mabhena, N., et al. (2022). Population Immunity and Covid-19
685 Severity with Omicron Variant in South Africa. N Engl J Med.

686 Meng, B., Abdullahi, A., Ferreira, I., Goonawardane, N., Saito, A., Kimura, I., Yamasoba, D.,
687 Gerber, P.P., Fatihi, S., Rathore, S., et al. (2022). Altered TMPRSS2 usage by SARS-CoV-2
688 Omicron impacts tropism and fusogenicity. Nature.

689 Nakamura, Y., Gojobori, T., and Ikemura, T. (2000). Codon usage tabulated from
690 international DNA sequence databases: status for the year 2000. Nucleic Acids Res 28,
691 292.

692 Nielsen, S.C.A., Yang, F., Jackson, K.J.L., Hoh, R.A., Roltgen, K., Jean, G.H., Stevens, B.A., Lee,
693 J.Y., Rustagi, A., Rogers, A.J., et al. (2020). Human B Cell Clonal Expansion and Convergent
694 Antibody Responses to SARS-CoV-2. Cell Host Microbe 28, 516-525 e515.

695 O'Brien, M.P., Forleo-Neto, E., Musser, B.J., Isa, F., Chan, K.C., Sarkar, N., Bar, K.J., Barnabas,
696 R.V., Barouch, D.H., Cohen, M.S., et al. (2021). Subcutaneous REGEN-COV Antibody
697 Combination to Prevent Covid-19. N Engl J Med 385, 1184-1195.

698 Perez-Then, E., Lucas, C., Monteiro, V.S., Miric, M., Brache, V., Cochon, L., Vogels, C.B.F.,
699 Malik, A.A., De la Cruz, E., Jorge, A., et al. (2022). Neutralizing antibodies against the SARS-
700 CoV-2 Delta and Omicron variants following heterologous CoronaVac plus BNT162b2
701 booster vaccination. Nat Med.

702 Pettersen, E.F., Goddard, T.D., Huang, C.C., Meng, E.C., Couch, G.S., Croll, T.I., Morris, J.H.,
703 and Ferrin, T.E. (2021). UCSF ChimeraX: Structure visualization for researchers,
704 educators, and developers. Protein Sci 30, 70-82.

705 Planas, D., Saunders, N., Maes, P., Guivel-Benhassine, F., Planchais, C., Buchrieser, J.,
706 Bolland, W.H., Porrot, F., Staropoli, I., Lemoine, F., et al. (2022). Considerable escape of
707 SARS-CoV-2 Omicron to antibody neutralization. Nature 602, 671-675.

708 Qassim, S.H., Chemaitelly, H., Ayoub, H., AlMukdad, S., Tang, P., Hasan, M.R., Yassine, H.M.,
709 Al-Khatib, H.A., Smatti, M.K., Abdul Rahim, H.F., et al. (2022). Effects of BA.1/BA.2
710 subvariant, vaccination, and prior infection on infectiousness of SARS-CoV-2 Omicron
711 infections. medRxiv.

712 Raybould, M.I.J., Kovaltsuk, A., Marks, C., and Deane, C.M. (2021). CoV-AbDab: the
713 coronavirus antibody database. Bioinformatics 37, 734-735.

714 Robbiani, D.F., Gaebler, C., Muecksch, F., Lorenzi, J.C.C., Wang, Z., Cho, A., Agudelo, M.,
715 Barnes, C.O., Gazumyan, A., Finkin, S., et al. (2020). Convergent antibody responses to
716 SARS-CoV-2 in convalescent individuals. Nature 584, 437-442.

717 Schmidt, F., Muecksch, F., Weisblum, Y., Da Silva, J., Bednarski, E., Cho, A., Wang, Z., Gaebler,
718 C., Caskey, M., Nussenzweig, M.C., et al. (2022). Plasma Neutralization of the SARS-CoV-2
719 Omicron Variant. N Engl J Med 386, 599-601.

720 Shu, Y., and McCauley, J. (2017). GISAID: Global initiative on sharing all influenza data -
721 from vision to reality. Euro Surveill 22.

722 Shuai, H., Chan, J.F., Hu, B., Chai, Y., Yuen, T.T., Yin, F., Huang, X., Yoon, C., Hu, J.C., Liu, H., et
723 al. (2022). Attenuated replication and pathogenicity of SARS-CoV-2 B.1.1.529 Omicron.
724 Nature.

725 Stothard, P. (2000). The sequence manipulation suite: JavaScript programs for analyzing
726 and formatting protein and DNA sequences. Biotechniques 28, 1102, 1104.

727 Tiller, T., Meffre, E., Yurasov, S., Tsuiji, M., Nussenzweig, M.C., and Wardemann, H. (2008).
728 Efficient generation of monoclonal antibodies from single human B cells by single cell RT-
729 PCR and expression vector cloning. J Immunol Methods 329, 112-124.

730 Tseng, H.F., Ackerson, B.K., Luo, Y., Sy, L.S., Talarico, C.A., Tian, Y., Bruxvoort, K.J., Tubert,
731 J.E., Florea, A., Ku, J.H., et al. (2022). Effectiveness of mRNA-1273 against SARS-CoV-2
732 Omicron and Delta variants. Nat Med.

733 VanBlargan, L.A., Errico, J.M., Halfmann, P.J., Zost, S.J., Crowe, J.E., Jr., Purcell, L.A., Kawaoka,
734 Y., Corti, D., Fremont, D.H., and Diamond, M.S. (2022). An infectious SARS-CoV-2 B.1.1.529
735 Omicron virus escapes neutralization by therapeutic monoclonal antibodies. Nat Med.

736 Vanshylla, K., Di Cristanziano, V., Kleipass, F., Dewald, F., Schommers, P., Gieselmann, L.,
737 Gruell, H., Schlotz, M., Ercanoglu, M.S., Stumpf, R., et al. (2021). Kinetics and correlates of
738 the neutralizing antibody response to SARS-CoV-2 infection in humans. Cell Host Microbe
739 29, 917-929 e914.

740 Vanshylla, K., Fan, C., Wunsch, M., Poopalasingam, N., Meijers, M., Kreer, C., Kleipass, F.,
741 Ruchnewitz, D., Ercanoglu, M.S., Gruell, H., et al. (2022). Discovery of ultrapotent broadly
742 neutralizing antibodies from SARS-CoV-2 elite neutralizers. Cell Host Microbe 30, 69-82
743 e10.

744 Viana, R., Moyo, S., Amoako, D.G., Tegally, H., Scheepers, C., Althaus, C.L., Anyaneji, U.J.,
745 Bester, P.A., Boni, M.F., Chand, M., et al. (2022). Rapid epidemic expansion of the SARS-
746 CoV-2 Omicron variant in southern Africa. Nature.

747 Weinreich, D.M., Sivapalasingam, S., Norton, T., Ali, S., Gao, H., Bhore, R., Xiao, J., Hooper,
748 A.T., Hamilton, J.D., Musser, B.J., et al. (2021). REGEN-COV Antibody Combination and
749 Outcomes in Outpatients with Covid-19. N Engl J Med 385, e81.

750 Weissman, D., Alameh, M.G., de Silva, T., Collini, P., Hornsby, H., Brown, R., LaBranche, C.C.,
751 Edwards, R.J., Sutherland, L., Santra, S., et al. (2021). D614G Spike Mutation Increases
752 SARS CoV-2 Susceptibility to Neutralization. Cell Host Microbe 29, 23-31 e24.

753 Wratil, P.R., Stern, M., Priller, A., Willmann, A., Almanzar, G., Vogel, E., Feuerherd, M.,
754 Cheng, C.C., Yazici, S., Christa, C., et al. (2022). Three exposures to the spike protein of
755 SARS-CoV-2 by either infection or vaccination elicit superior neutralizing immunity to all
756 variants of concern. Nat Med.

757 Yamasoba, D., Kimura, I., Nasser, H., Morioka, Y., Nao, N., Ito, J., Uriu, K., Tsuda, M.,
758 Zahradnik, J., Shirakawa, K., et al. (2022). Virological characteristics of SARS-CoV-2 BA.2
759 variant. medRxiv.

760 Ye, J., Ma, N., Madden, T.L., and Ostell, J.M. (2013). IgBLAST: an immunoglobulin variable
761 domain sequence analysis tool. Nucleic Acids Res 41, W34-40.

762 Yuan, M., Liu, H., Wu, N.C., Lee, C.D., Zhu, X., Zhao, F., Huang, D., Yu, W., Hua, Y., Tien, H., et
763 al. (2020). Structural basis of a shared antibody response to SARS-CoV-2. Science 369,
764 1119-1123.

765 Zhang, Q., Ju, B., Ge, J., Chan, J.F., Cheng, L., Wang, R., Huang, W., Fang, M., Chen, P., Zhou, B.,
766 et al. (2021). Potent and protective IGHV3-53/3-66 public antibodies and their shared
767 escape mutant on the spike of SARS-CoV-2. Nat Commun 12, 4210.

768 Zhao, X., Li, D., Ruan, W., Chen, Z., Zhang, R., Zheng, A., Qiao, S., Zheng, X., Zhao, Y., Dai, L.,
769 et al. (2022). Effects of a Prolonged Booster Interval on Neutralization of Omicron Variant.
770 N Engl J Med 386, 894-896.

771

Figure 1

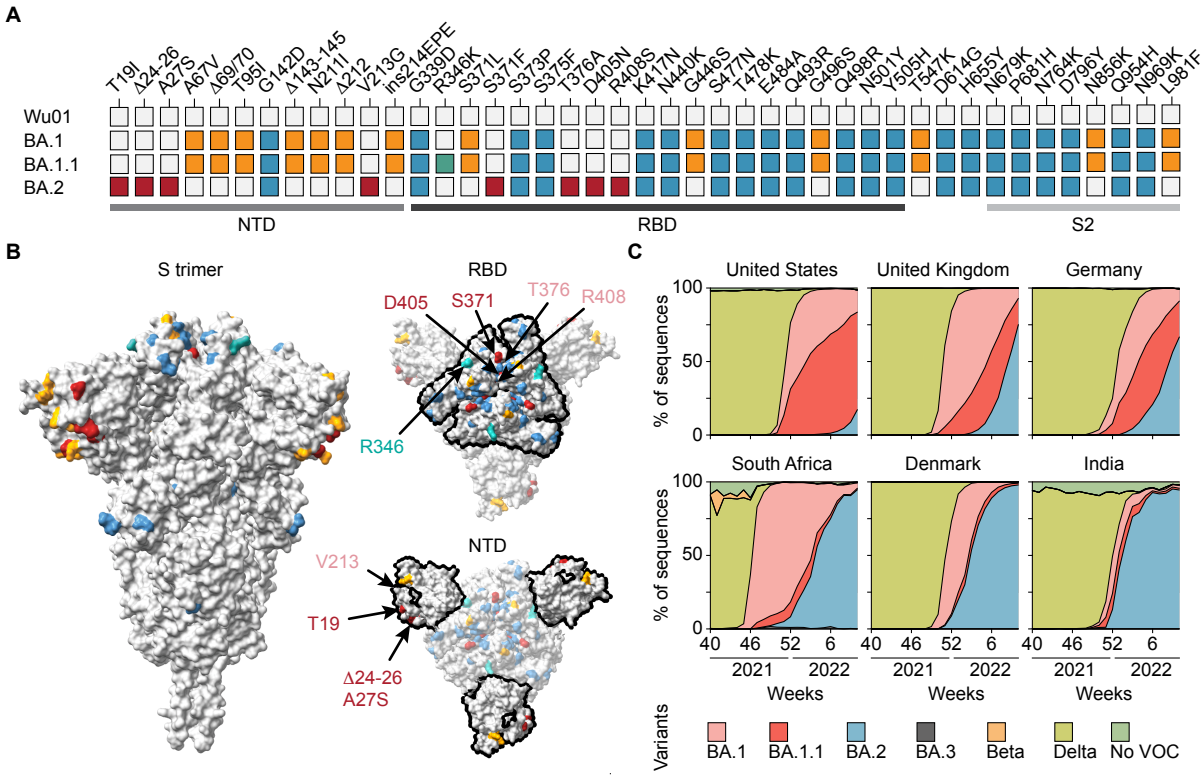

Figure 1. Omicron sublineage differences.
(A) Spike amino acid changes in the BA.1, BA.1.1, and BA.2 Omicron sublineages relative to Wu01. **(B)** Locations of changed amino acids in Omicron sublineages highlighted on the SARS-CoV-2 spike (PDB: 6XR8). Representations on the right show RBD and NTD outlined in black. Changes exclusive to BA.2 are indicated in dark red (visible on surface) and light red (not visible). In (A) and (B), mutations shared between BA.1 and BA.1.1 are shown in orange, mutations shared between BA.1, BA.1.1 and BA.2 are shown in blue, the R346K mutation exclusive to BA.1.1 is shown in green, and mutations exclusive to BA.2 are shown in red. **(C)** Proportion of sequences submitted to the GISAID SARS-CoV-2 database per variant and week (accessed on April 2, 2022). NTD, N-terminal domain; RBD, receptor-binding domain; PDB, Protein Data Bank.

Figure 2

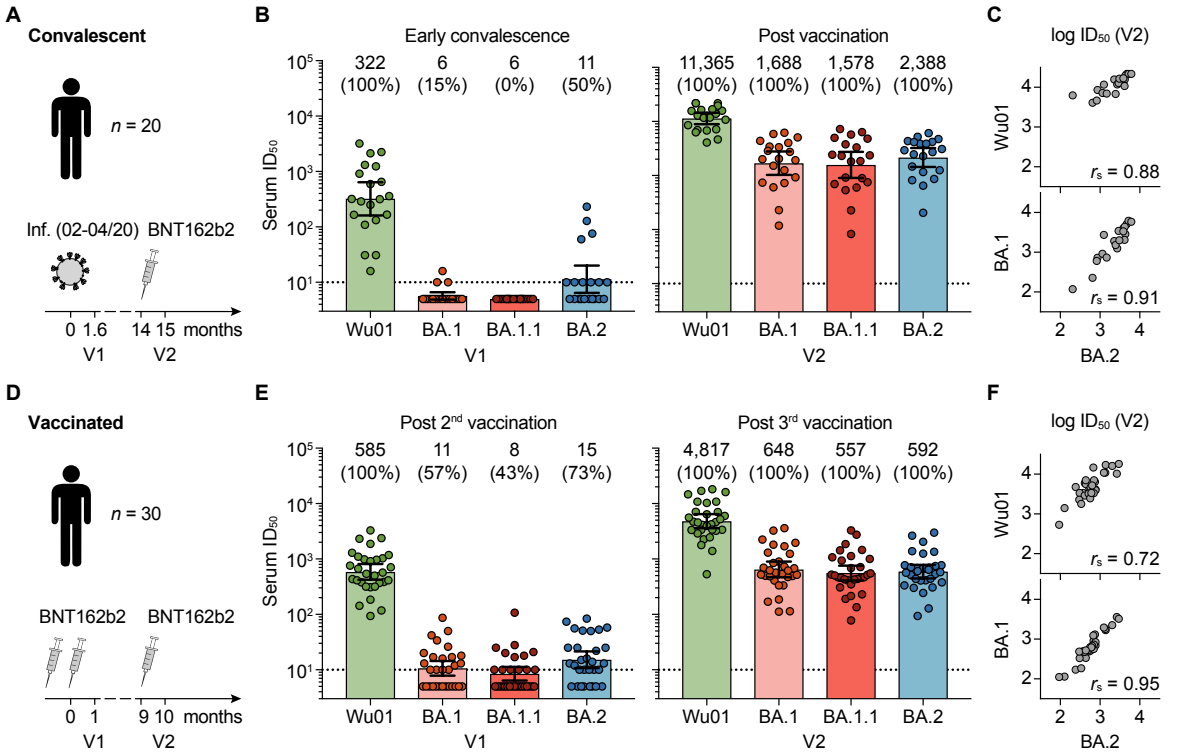

Figure 2. Omicron sublineage-neutralizing serum activity in vaccinated and convalescent individuals.
(A) Study scheme in COVID-19-convalescent individuals. Samples were collected after infection occurring between February and April, 2020 (V1), and after a BNT162b2 booster immunization (V2). **(B)** Fifty-percent inhibitory serum dilutions (ID_{50}s) against Wu01, BA.1, BA.1.1, and BA.2 determined by pseudovirus neutralization assays in convalescent individuals. Bars indicate geometric mean ID_{50}s with 95% confidence intervals (CIs) at V1 (left) and V2 (right). Numbers indicate geometric mean ID_{50}s and percentage of individuals with detectable neutralizing activity (ID_{50} >10) in parentheses. **(C)** Correlation plots of log_{10} serum ID_{50}s against Wu01 (top) and BA.1 (bottom) versus BA.2 at V2 in convalescent individuals. r_s indicates Spearman's rank correlation coefficients. **(D)** Study scheme in vaccinated individuals. Samples were collected after the second dose of BNT162b2 (V1) and after the third dose of BNT162b2 (V2). **(E)** Serum ID_{50}s against Wu01, BA.1, BA.1.1, and BA.2 determined by pseudovirus neutralization assays in vaccinated individuals. Bars indicate geometric mean ID_{50}s with 95% CIs at V1 (left) and V2 (right). Numbers indicate geometric mean ID_{50}s and percentage of individuals with detectable neutralizing activity (ID_{50} >10) in parentheses. **(F)** Correlation plots of log_{10} serum ID_{50}s against Wu01 (top) and BA.1 (bottom) versus BA.2 at V2 in vaccinated individuals. r_s indicates Spearman's rank correlation coefficients. In (B) and (E), ID_{50}s below the lower limit of quantification (LLOQ, ID_{50} of 10; indicated by black dotted lines) were imputed to ½ LLOQ (ID_{50}=5). In (B) and (C), ID_{50}s above the upper limit of quantification (21,870) were imputed to 21,871.

Figure 3

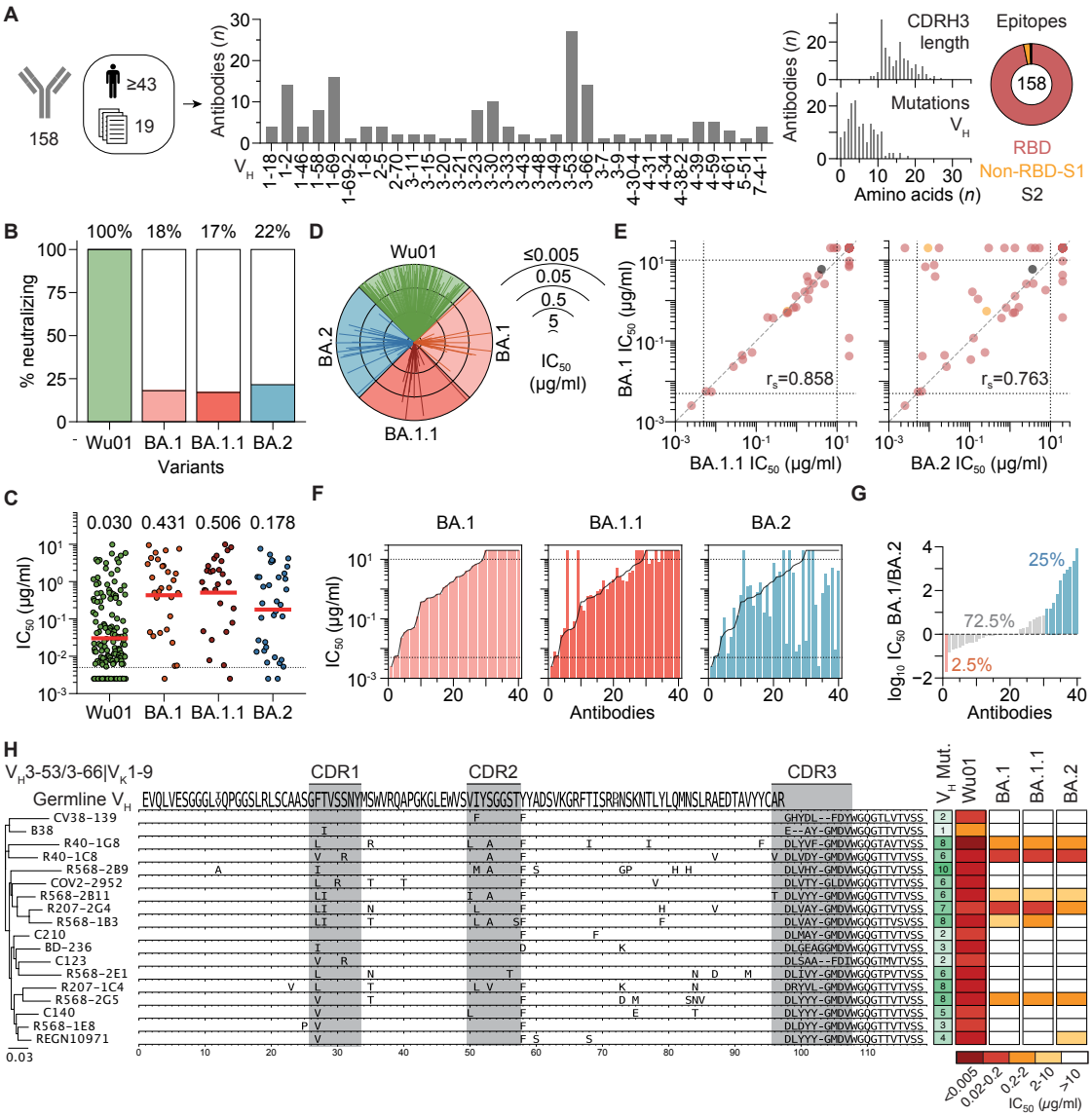

Figure 3. Determining Omicron sublineage immune escape using monoclonal antibodies.
(A) SARS-CoV-2-neutralizing monoclonal antibodies (n=158) derived from 19 studies and isolated from ≥43 convalescent individuals were analyzed. Bar charts indicate number of antibodies per heavy chain variable gene segment (V_H), amino acid (aa) length of the heavy chain complementarity-determining region 3 (CDRH3), and number of V_H aa mutations relative to the V_H germline gene. Pie chart indicates antibody epitopes with slice sizes proportional to the number of antibodies. **(B)** Fraction of monoclonal antibodies neutralizing (IC_{50} <10 µg/ml) Wu01 (green), BA.1 (light red), BA.1.1 (dark red), and BA.2 (blue) in pseudovirus neutralization assay. **(C)** IC_{50}s of antibodies with neutralizing activity (IC_{50} <10 µg/ml) against the individual variants (Wu01, n=158; BA.1, n=29; BA.1.1, n=27; BA.2, n=34). Bars depict geometric mean IC_{50}s and dotted line indicates lower limit of quantification (LLOQ, 0.005 µg/ml). **(D)** Spider plot of IC_{50}s for all antibodies against Wu01, BA.1, BA.1.1, and BA.2. Antibodies are sorted arbitrarily but equally for each virus. **(E)** Correlation plots of IC_{50}s of all antibodies against BA.1.1 (left) and BA.2 (right) versus BA.1. Colors indicate epitopes as in (A). Dashed lines represent identity lines and dotted lines indicate limits of quantification. **(F)** Bar charts of antibodies with neutralizing activity (IC_{50} <10 µg/ml) against any Omicron sublineage (n=40). Antibodies in each chart are sorted by BA.1-neutralizing activity (black outline) and bars show IC_{50}s against indicated sublineages. Dotted lines show LLOQ (0.005 µg/ml) and upper limit of quantification (ULOQ; 10 µg/ml). **(G)** Ratio (log_{10}) of IC_{50}s against BA.1 and BA.2 for all neutralizing antibodies with any Omicron sublineage-neutralizing activity (IC_{50} <10 µg/ml; n=40). Ratios >1 log_{10} are highlighted in green and percentage of antibodies with ratio >1 log_{10} is indicated. In (E)-(G), IC_{50} <LLOQ were imputed to ½ LLOQ (IC_{50}=0.0025) and IC_{50} values >ULOQ were imputed to 2x ULOQ (IC_{50}=20). **(H)** Phylogenetic tree and sequence alignment of antibodies of the V_H3-53/3-66|V_K1-9 public clonotype. Letters indicate aa mutations relative to the V_H germline gene. Number of aa mutations compared to the corresponding germline allele and neutralizing activity against Wu01, BA.1, BA.1.1, and BA.2 are indicated on the right. Germline V_H represents the consensus of all identified germline alleles of depicted antibodies (VH3-53*01, VH3-53*04, and VH3-66*01).

Figure 4

A

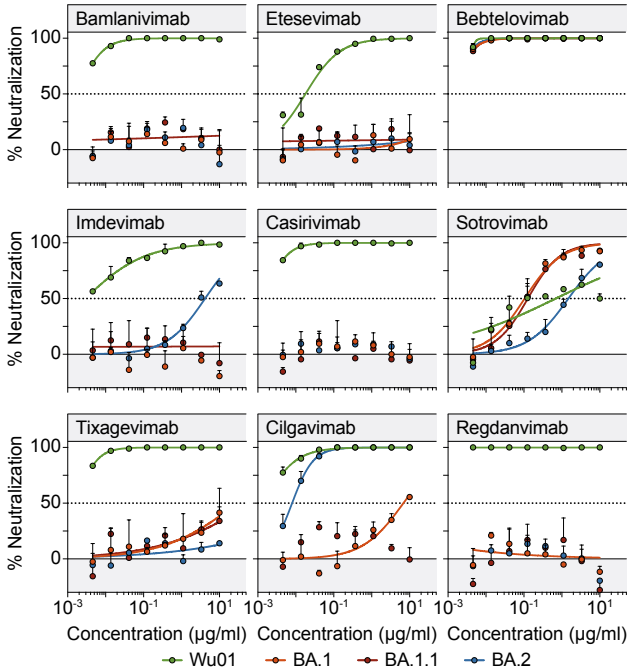

B

	Antibody		IC_{50} (µg/ml)			
	Clinical ID	Parental ID	Wu01	BA.1	BA.1.1	BA.2
Approved	Bamlanivimab*	LY-CoV555	<0.005	>10	>10	>10
	Etesevimab*	CB6/JS016	0.018	>10	>10	>10
	Bebtelovimab	LY-CoV1404†	<0.005	<0.005	<0.005	<0.005
	Imdevimab*	REGN10987	<0.005	>10	>10	4.173
	Casirivimab*	REGN10933	<0.005	>10	>10	>10
	Sotrovimab*	S309	0.685	0.105	0.127	1.488
	Tixagevimab	COV2-2196†	<0.005	>10	>10	>10
	Cilgavimab	COV2-2130†	<0.005	6.848	>10	0.008
	Regdanvimab	CT-P59†	<0.005	>10	>10	>10
In trials	DZIF-10c*	HbnC3t1p1_F4	<0.005	0.046	>10	0.033
	BRII-196	P2C-1F11†	<0.005	>10	>10	>10
	BMS-986414	C135†	<0.005	>10	>10	>10
	BMS-986413	C144†	<0.005	>10	>10	>10
	ADM03820§	COV2-2381†	0.008	>10	>10	>10
	ADG-20	ADG-2†	<0.005	0.212	0.194	>10
	ABBV-47D11	47D11†	0.386	>10	>10	>10
	BGB-DXP593	BD-368-2†	<0.005	>10	>10	>10
	n.a.	MAD0004J08†	<0.005	>10	>10	>10

* Clinical product used.
† Parental antibody (Fc-unmodified IgG1) used.
§ Combination product of COV2-2381 and COV2-2130.

Figure 4. Omicron sublineage-neutralizing activity of monoclonal antibodies in clinical use.
(A) Dose response curves showing % neutralization of monoclonal antibodies against Wu01, BA.1, BA.1.1, and BA.2 in pseudovirus neutralization assay. Circles show averages and error bars indicate standard deviation. Dotted lines indicate 50% neutralization (IC_{50}). **(B)** IC_{50}s against Wu01, BA.1, BA.1.1, and BA.2 of monoclonal antibodies with current or previous authorization for clinical use or in clinical development. Symbols indicate whether clinical products or parental antibodies produced as human IgG1 were used.